Quantifying pesticide emissions for drift deposition in comparative risk and impact assessment

Zhang, Yuyue; Li, Zijian; Reichenberger, Stefan; Gentil-Sergent, Céline; Fantke, Peter

Published in:
Environmental Pollution

Link to article, DOI:
10.1016/j.envpol.2023.123135

Publication date:
2024

Document Version
Publisher's PDF, also known as Version of record

Environmental Pollution 342 (2024) 123135

Contents lists available at ScienceDirect

Environmental Pollution

journal homepage: www.elsevier.com/locate/envpol

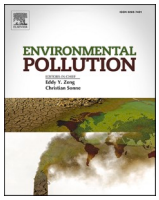

Quantifying pesticide emissions for drift deposition in comparative risk and impact assessment☆

Yuyue Zhang [a,*], Zijian Li [b], Stefan Reichenberger [c], Céline Gentil-Sergent [d,e], Peter Fantke [a,f]

[a] Quantitative Sustainability Assessment, Department of Environmental and Resource Engineering, Technical University of Denmark, Bygningstorvet 115, 2800, Kgs. Lyngby, Denmark
[b] School of Public Health (Shenzhen), Sun Yat-sen University, Guangdong, 518107, China
[c] knoell France SAS, 5 rue Gorge de Loup, 69009, Lyon, France
[d] CIRAD, UPR HortSys, ELSA, F-97232, Le Lamentin, Martinique, France
[e] Santé Publique France (SpF), F-94415, Saint-Maurice, France
[f] Centre for Absolute Sustainability, Technical University of Denmark, Bygningstorvet 115, 2800 Kgs. Lygnby, Denmark

ARTICLE INFO

Keywords:
Spray drift
Drift experiments
Chemical pollution
Plant protection products
Emission modelling

ABSTRACT

Estimating emissions of chemical pesticides used in agriculture is an essential component in evaluating the potential toxicity-related impacts on humans and ecosystems in various comparative risk and impact assessment frameworks, such as life cycle assessment, environmental footprinting, absolute environmental sustainability assessment, chemical substitution, and risk prioritization. Emissions related to drift deposition—usually derived from drift experiments—can reach non-target areas, and vary as a function of crop characteristics and application technique. We derive cumulative drift deposition fractions for a wide range of experimental drift functions for use in comparative and mass-balanced approaches. We clarify that cumulative drift deposition fractions require to integrate the underlying drift functions over the relevant deposition area and to correct for the ratio of deposition area to treated field area to arrive at overall mass deposited per unit mass of applied pesticide. Our results show that for most crops, drift deposition fractions from pesticide application are below 0.03 (i.e. 3% of applied mass), except for grapes and fruit trees, where drift fractions can reach 5% when using canon or air blast sprayers. Notably, aerial applications on soybeans can result in significantly higher drift deposition fractions, ranging from 20% to 60%. Additionally, varying the nozzle position can lead to a factor of five differences in pesticide deposition, and establishing buffer zones can effectively reduce drift deposition. To address remaining limitations in deriving cumulative drift deposition fractions, we discuss possible alternative modelling approaches. Our proposed approach can be implemented in different quantitative and comparative assessment frameworks that require emission estimates of agricultural pesticides, in support of reducing chemical pollution and related impacts on human health and the environment.

1. Introduction

Evaluating toxicity-related impacts of chemical emissions on humans and ecosystems is an integral part of environmental management and environmental performance assessments of products and technologies (Fantke et al., 2018a, 2018b). Such information is relevant for life cycle assessment (LCA), environmental footprinting, chemical substitution, exposure and risk prioritization, and absolute environmental sustainability assessment (AESA) (Aurisano et al., 2021; Fantke et al., 2021, 2020; Fantke and Illner, 2019; Hauschild et al., 2018; Jolliet et al., 2021; Kosnik et al., 2022; Owsianiak et al., 2023; Persson et al., 2022; Tarasova et al., 2018; von Borries et al., 2023; Zijp et al., 2014). As part of evaluating toxicity-related impacts, emissions associated with chemical pesticides applied to agricultural fields for producing food, fodder, biofuel or other crops can be estimated by mass balance approaches using applied pesticide mass on a given field area as a starting point (Nemecek et al., 2022).

Drift deposition is one of the main processes that drives how field-applied pesticide mass distributes in the environment. It can be influenced by field management practices, such as using drift reduction

☆ This paper has been recommended for acceptance by Prof. Pavlos Kassomenos.

* Corresponding author.
E-mail address: yuyzh@dtu.dk (Y. Zhang).

https://doi.org/10.1016/j.envpol.2023.123135
Received 27 July 2023; Received in revised form 27 November 2023; Accepted 8 December 2023
Available online 11 December 2023

technologies, to protect primarily natural vegetation and water surfaces outside agricultural field areas (Gentil-Sergent et al., 2021; Reichenberger et al., 2007). Drift deposition is thereby frequently referred to as 'drift'. This term, however, can be misleading as it includes both the fraction of applied pesticide mass that remains airborne after undergoing wind drift (i.e. airborne emissions to air) and the fraction of applied mass that is deposited on surface areas after undergoing wind drift, typically considering surface areas outside a treated field itself (i.e. drift deposition-related emissions to off-field surfaces) (ISO, 2005). To estimate drift deposition, current pesticide emission models, such as PestLCI, directly apply different types of power or exponential functions that were themselves derived from fitting measured drift deposition results for a given combination of crop or crop type and application method (FOCUS, 2001; García-Santos et al., 2016; Holterman et al., 2017; Rautmann et al., 2001; van de Zande et al., 2015).

Drift deposition results are used in several decision contexts to derive cumulative emission fractions over a given deposition area, based on applying the underlying drift deposition functions to multiple spray swaths and interpreting related results as mass fraction of applied pesticide that is deposited outside a treated field area (Birkved and Hauschild, 2006; Dijkman et al., 2012; Renaud-Gentié et al., 2015; Tang et al., 2020). However, drift deposition functions provide point estimates at a given distance as commonly applied in ecological risk assessment and environmental protection, while a cumulative estimate is needed when characterizing emissions from a certain pesticide application in terms of their toxicity-related impacts on the environment. Furthermore, drift deposition results refer via a single function (i.e. for a given crop/crop type-application method combination) to a sufficiently large number of spray swaths ($n \geq 1$) applied over a given treated field area to ensure that the contribution of any additional swath to deposition mass is negligible. The exception are single-swath experiments that aim to evaluate the contribution of each spray swath to an overall deposition mass (Holterman et al., 2018). Finally, drift deposition results based on spray experiments are usually given in units that link the mass deposited per unit deposition area to a unit mass of pesticide applied per unit treated field area. See for example van de Zande et al., (2015) for additional details on these aspects. Studies that do not account for these aspects will yield cumulative emission distribution results that cannot be correctly interpreted in the context of evaluating the environmental performance of agricultural practices in various decision-making contexts that are based on overall emission mass per scenario.

To provide guidance on these aspects, we will clarify in the present study how to properly interpret and implement the wider range of measurement-based drift deposition functions in mass balance approaches for estimating cumulative pesticide emissions. More specifically, we will clarify three points, which we implemented into the PestLCI Consensus web-tool (Nemecek et al., 2022). (1) Drift deposition functions need to be integrated over the relevant deposition area. (2) Drift deposition functions need to be applied only once per pesticide application scenario and not per spray swath. (3) Drift deposition results need to be corrected for the ratio of deposition area to treated field area to arrive at mass deposited per unit mass of applied pesticide. Finally, we provide an overview of possible alternative approaches for estimating drift deposition related emissions, which address some of the current limitations when deriving such emissions from specific drift functions. Our guidance aims at aiding practitioners to derive and interpret cumulative pesticide emissions for application in quantitative and comparative assessment frameworks.

2. Methods

2.1. Deposition-related emission fraction

The impact score for a given product system for toxicity-related impacts of field-applied pesticide emissions, *IS* (impact/functional unit), is derived as:

$$IS = \sum_{p,c} CF_{p,c} \times \overbrace{m_{\mathrm{app},p,c} \times f_c}^{m_{\mathrm{emi},p,c}} \quad (1)$$

where $m_{\mathrm{emi},p,c}$ [$kg_{emitted}$/functional unit] is the total emitted mass of pesticide p emitted into a given environmental compartment c, and $CF_{p,c}$ [impact/$kg_{emitted}$] is the corresponding characterization factor for a given impact category (i.e. human toxicity or ecotoxicity). Emission mass is typically not known, but can be obtained from (a) the total applied pesticide mass for a given field or application scenario, $m_{\mathrm{app},p,c}$ [$kg_{applied}$/functional unit], reported or found e.g. in agricultural statistics, and (b) the related mass fraction that is emitted into the environment, f_c [$kg_{emitted}/kg_{applied}$], defined as the fraction of mass applied to the treated field [$kg_{applied}$] that reaches the different environmental compartments as emission [$kg_{emitted}$]. Applied mass can alternatively be derived from reported pesticide doses applied to a certain area, and aggregated over various treatments, where differences in application method and crop growth stages need to be appropriately considered as they influence emission patterns (Gentil-Sergent et al., 2021; Gentil et al., 2020b; Rosenbaum et al., 2015).

In the different versions of the PestLCI model, emission fractions f_c are available for pesticide mass reaching air, field crop and field soil, and off-field areas (i.e. those areas outside the boundaries of the treated agricultural field under study). Emission fractions related to those off-field areas (including agricultural soil of adjacent fields, natural and other soil, and water surfaces) are derived from the pesticide mass fraction deposited in areas outside the treated field, which by assumption is located in downwind direction. This deposited mass can be obtained from drift deposition measurements, which provide the mass deposited in an area unit within the deposition area per mass applied to an area unit of the treated field. With that, the drift deposition experiments deliver a fraction of area-based mass densities, $f(x) = \rho_{A,\mathrm{dep}} / \rho_{A,\mathrm{app}}$ [$kg_{deposited}/m^2_{deposition\ area}$ per $kg_{applied}/m^2_{treated\ field\ area}$] at a given distance x from the boundary between the treated field and the off-field deposition area (the so-called field edge), which we can also denote a 'deposition dose fraction'. Since in different decision-making contexts, we want to calculate the cumulative mass deposited in the off-field deposition area per unit mass applied in the treated field area, the results of the drift deposition experiments need to be translated into a deposition-related mass fraction f_{dep} [$kg_{deposited}/kg_{applied}$]. The off-field area can consist of different compartments c, each of which would get an area share S_c [$m^2_{compartment}/m^2_{total\ off\text{-}field}$]. From that, we can integrate f_{dep} into eq. (1) to derive emission fractions into specific off-field area-related compartments for drift deposition as:

$$f_c = f_{\mathrm{dep}} \times S_c \quad (2)$$

2.2. General and integral forms of reported drift deposition functions

For different crops and following different drift deposition test protocols, various forms of fitted drift deposition functions, namely, $f(x)$ [kg/m^2 per kg/m^2], are commonly proposed. A list of the most widely applied drift deposition functions used in emission modelling is provided in the following:

$$f(x) = \alpha \times x^{\beta} \quad (3a)$$

(e.g. Rautmann et al., 2001; FOCUS, 2001)

$$f(x) = \alpha_1 \times x^{\beta_1} + \alpha_2 \times x^{\beta_2} \quad (3b)$$

(generalization of eq. (3a))

$$f(x) = (\alpha + \beta \times x^2)^{-1} \quad (3c)$$

(e.g. Hernández-Hernández et al., 2007)

$$f(x) = \alpha_1 \times e^{\beta_1 \times x} + \alpha_2 \times e^{\beta_2 \times x} \tag{3d}$$

(e.g. Holterman and van de Zande, 2003)

$$f(x) = \alpha \times \ln(x) + \beta \tag{3e}$$

(e.g. Gouda et al., 2018)

$$f(x) = \begin{cases} \alpha_1 \times x^{\beta_1} \text{ for } 0 \leq x \leq H \\ \alpha_2 \times x^{\beta_2} \text{ for } x > H \end{cases} \tag{3f}$$

(e.g. Rautmann et al., 2001; FOCUS, 2001).Where α and β are fitting parameters, and H is the hinge point (or breakpoint) defining the distance limit for each regression in the so-called "hockey stick" model, which consists of two sequential curves. However, the hockey stick model has no specific advantage as compared to other bi-phasic models (e.g. eqs. (3b) and (3d)) regarding the description of drift deposition kinetics.

In order to calculate the cumulated emission mass fraction of the pesticide in the off-field drift deposition area, any fitted drift deposition function needs to be integrated over the deposition distance. The general integral form of any drift deposition function is given as:

$$F(x) = \int_{x_1}^{x_2} f(x)\, dx \tag{4}$$

where x (m) denotes the relevant deposition distance. Since we want to integrate over a specific distance, we need to derive the definite integral over distance between $x_1 = 0$ (i.e. field edge) and $x_2 = z_2$ (drift deposition function-specific largest defined distance from the field edge in downwind direction, which corresponds to the upper validity limit of a drift deposition function, z_2). With $x_1 = 0$, this distance is defined as $x_2 - x_1 = x_2$. Dividing the generalized form in eq. (4) by distance x_2 yields a 'mean cumulative deposition dose fraction' in the given deposition area with unit $kg_{deposited}/\ m^2_{deposition\ area}$ per $kg_{applied}/\ m^2_{treated\ field\ area}$ as (Bach et al., 2017; EFSA, 2020; FOCUS, 2001):

$$\bar{f}_{[x_1,x_2]} = \frac{F(x)}{x_2} = \frac{1}{x_2} \times \int_{x_1}^{x_2} f(x)\, dx \tag{5}$$

Applying eq. (5) to the example set of drift deposition functions in eq. (3) then yields:

$$\bar{f}_{[x_1,x_2]} = \left[\frac{\alpha}{\beta+1} \times \left({x_2}^{\beta+1} - {x_1}^{\beta+1}\right)\right] \times \frac{1}{x_2} \tag{6a}$$

$$\bar{f}_{[x_1,x_2]} = \left[\frac{\alpha_1}{\beta_1+1} \times \left({x_2}^{\beta_1+1} - {x_1}^{\beta_1+1}\right) + \frac{\alpha_2}{\beta_2+1} \times \left({x_2}^{\beta_2+1} - {x_1}^{\beta_2+1}\right)\right] \times \frac{1}{x_2} \tag{6b}$$

$$\bar{f}_{[x_1,x_2]} = \left[\frac{1}{\sqrt{\alpha \times \beta}} \times \arctan\left(\sqrt{\frac{\beta}{\alpha}} \times x_2\right) - \frac{1}{\sqrt{\alpha \times \beta}} \times \arctan\left(\sqrt{\frac{\beta}{\alpha}} \times x_1\right)\right] \times \frac{1}{x_2}, \alpha, \beta > 0 \tag{6c}$$

$$\bar{f}_{[x_1,x_2]} = \left[\frac{\alpha_1}{\beta_1} \times \left(e^{\beta_1 \times x_2} - e^{\beta_1 \times x_1}\right) + \frac{\alpha_2}{\beta_2} \times \left(e^{\beta_2 \times x_2} - e^{\beta_2 \times x_1}\right)\right] \times \frac{1}{x_2} \tag{6d}$$

$$\bar{f}_{[x_1,x_2]} = [\alpha \times x_2 \times \ln(x_2) - \alpha \times x_1 \times \ln(x_1) + (\beta - \alpha) \times (x_2 - x_1)] \times \frac{1}{x_2} \tag{6e}$$

$$\bar{f}_{[x_1,x_2]} = \left[\frac{\alpha_1}{\beta_1+1} \times \left(H^{\beta_1+1} - {x_1}^{\beta_1+1}\right) + \frac{\alpha_2}{\beta_2+1} \times \left({x_2}^{\beta_2+1} - H^{\beta_2+1}\right)\right] \times \frac{1}{x_2} \tag{6f}$$

We note that eq. (6f) simplifies to eq. (6a) if the furthest distance of the deposition area x_2 is less than the hinge distance H.

2.3. Considerations for obtaining the mean deposition fraction

When dealing with real-world scenarios, most spray nozzles will be located inside the treated field, while the last nozzles of a spray swath near the field edge can be located either inside or outside the treated field. In these different cases of the position of the last spray nozzles (hereafter referred to as "spray nozzles" for simplicity), the mean deposition fraction cannot be directly derived from the experimental drift deposition function. For example, when the spray nozzles are located outside the treated field, utilizing an experimental drift deposition function can lead to an underestimation of the pesticide deposition. On the other hand, if the spray nozzles are located at a particular distance from the field edge within the treated field, using an experimental drift deposition function can result in an overestimation of the deposition fraction.

While the spray nozzle position is a practical consideration, experimental drift deposition functions also have an upper and a lower validity limit, i.e. they are not valid for very large or short deposition distances. The far edge, z_2, usually denotes the deposition area length beyond which additional deposition is negligible, as determined by the underlying drift experiments. However, at the short end, z_1, (i.e. limit close to the field edge), the deposition calculated by a given drift function could be very high due to the power law or exponential nature of such functions. Drift functions are usually estimated from experimental data, based on measuring the amount of pesticide deposited in the off-field area. However, the mathematical functions used to estimate drift deposition may yield extremely high values between the field edge ($x = 0$) and the lower validity limit of a drift function ($x = z_1$). To address this issue, the default value of the drift deposition fraction below the lower validity limit is set to $f^{max} = 1$ (i.e. 100%), which is consistent with the experimental settings. The drift deposition function with considerations of the curve's validity limits can be described as:

$$\bar{f}_{[x_1,x_2]} = \bar{f}_{[0,z_2]} = \frac{z_1 \times f^{max}_{[0,z_1]} + z_2 \times \bar{f}_{[z_1,z_2]}}{z_2} \tag{7}$$

Depending on the location of the spray nozzles in relation to the field edge, the starting point of drift deposition can be located inside the field, at the field edge or outside the field. Here, the assumption is made that the starting point of drift deposition is located at the spray nozzle position. The three cases for relating deposition-related distance x to the intrinsic integration boundaries z of the drift deposition function with consideration of the function's intrinsic validity limits are illustrated in Fig. 2 and can mathematically be described as follows:

$$\bar{f}_{[x_1,x_2]} = \begin{cases} \bar{f}_{[0,z_2]} \text{ for } x_n = 0 \text{ (spray nozzles at field edge)} \\ \bar{f}_{[0,z_2]} - \dfrac{|x_n| \times \bar{f}_{[0,|x_n|]}}{z_2} \text{ for } x_n < 0 \text{ (spray nozzles inside the field)} \\ \bar{f}_{[0,z_2]} + \dfrac{x_n \times f^{max}_{[0,x_n]}}{z_2} \text{ for } x_n > 0 \text{ (spray nozzles outside the field)} \end{cases} \tag{8}$$

2.4. Deriving the final drift deposition fraction

From the mean cumulative drift deposition fraction, we derive the cumulative deposited mass in the deposition area, m_{dep} [$kg_{deposited}$], as:

$$m_{dep} = \bar{f}_{[x_1,x_2]} \times A_{dep} \times D_{app} \tag{9}$$

with $A_{dep} = l_{[x_1,x_2]} \times w_{field}$ [$m^2_{deposition\ area}$] denoting the off-field deposition area in downwind direction from the treated field, where $l_{[x_1,x_2]}$ [m] is the distance between the field edge and the upper limit of the deposition-related, drift deposition function-specific integral, and w_{field} [m] is the field width parallel to the field edge, and with D_{app} [$kg_{applied}/\ m^2_{treated\ field\ area}$] denoting the pesticide application dose. The mass fraction deposited, f_{dep}, in units kg deposited/kg applied can finally be derived as:

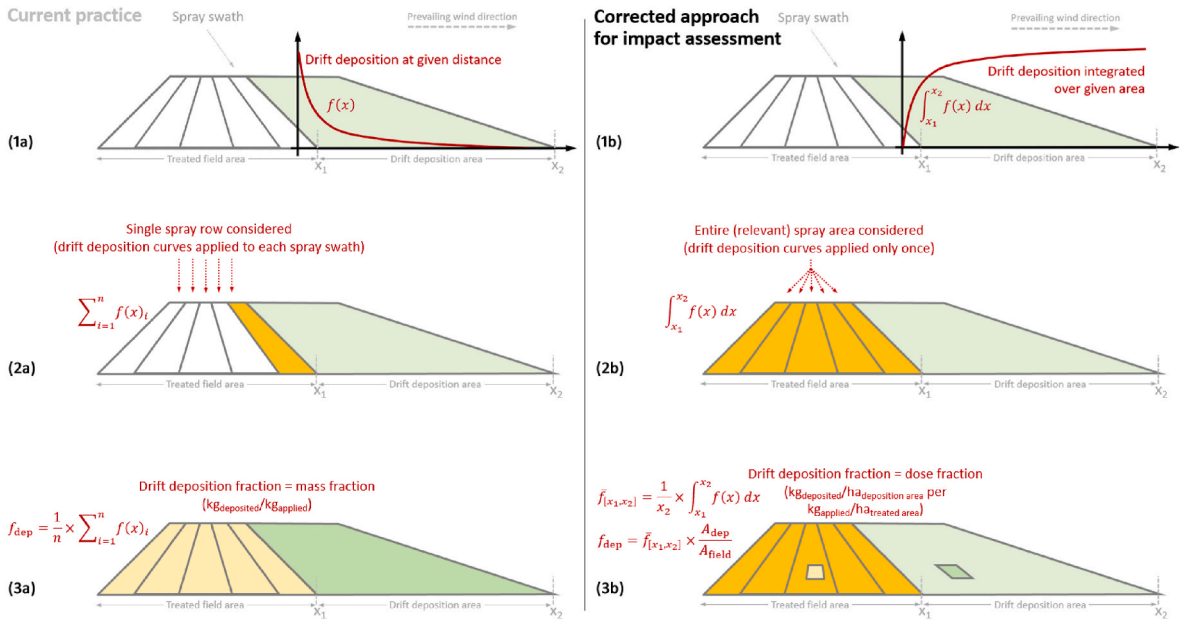

Fig. 1. Illustration of three conceptual aspects currently prevailing in some pesticide emission models (left side), and how we propose to correct these aspects for appropriate use in impact assessment contexts requiring cumulative emission fractions (right side). All aspects are discussed in detail in the text and in the Supplementary Material, Table S1.

$$f_{dep} = \frac{m_{dep}}{D_{app} \times A_{field}} = \overline{f}_{[x_1,x_2]} \times \frac{A_{dep}}{A_{field}} \quad (10)$$

with $A_{field} = l_{field} \times w_{field}$ [$m^2_{treated\ field\ area}$] denotes the agricultural field area relevant for the studied pesticide application, where l_{field} [m] is the field length perpendicular to the field edge, and w_{field} [m] is the field width parallel to the field edge. We can finally substitute f_{dep} in eq. (2) by eq. (10) to derive direct emission fractions into off-field surface areas associated with drift deposition. Note that in all original drift deposition functions that express results as fraction (dimensionless), the coefficients have been adapted to yield a true fraction.

2.5. Model application

We used existing reported drift functions to determine cumulative drift deposition fractions that can be utilized in pesticide emission models within LCA, environmental footprinting and elsewhere. Ten relevant studies were included from which we extracted 44 commonly used drift functions, taking into account the median or mean experimental drift deposition results. These drift functions represent diverse crop categories, regions, and application methods, including soybeans, olives, cotton, grapes/vines, cereals, fruit trees, and other permanent crops in Europe, Mexico, Benin, and Brazil. Considered application methods include boom sprayer, aerial application, hand-operated application, and air blast sprayer, with various drift reduction techniques using different nozzle or fan types (further details are found in the Supplementary Material, Table S2).

The selected drift functions can be assigned to their general forms in eq. (3). Their respective integral forms in eq. (6) can be directly used or implemented by users to derive cumulative drift deposition fractions for various pesticide application scenarios according to eqs. (7)–(10), with lower and upper validity limits of each drift function being considered (example calculation detailed in Supplementary Material, S1.1). The final mass deposition fraction is influenced by both the deposition area and field area; hence, various length-width ratios of a rectangular field shape were tested. Additionally, a comparison was conducted between the drift deposition fraction based on cumulative mass and point estimates that were used in a previous study.

We also tested the effect of the position of the spray nozzles (x_n) on estimated pesticide deposition mass (m_{dep}), using the deposition mass ratio, $r_{dep,mass}(x_n)$, of the real-world scenario and the optimal 'spray nozzles at field edge' scenario as an example:

$$r_{dep,mass}(x_n) = \frac{m_{dep,real}(x_n)}{m_{dep,empirical}} = \frac{m_{dep,real}(x_n)}{m_{dep,real}(0)} \quad (11)$$

where $m_{dep,real}(x_n)$ denotes the estimated m_{dep} value for the real-world scenario, which is a function of x_n; $m_{dep,empirical}$ denotes the estimated m_{dep} value for the default scenario with drift deposition starting at field edge (i.e. $x_n = 0$), which equals $m_{dep,real}(0)$. Based on eq. (8), $r_{dep,mass}(x_n)$ can be expressed as follows:

$$r_{dep,mass}(x_n) = \begin{cases} 1 \text{ for } x_n = 0 \text{ (spray nozzles at field edge)} \\ 1 - \dfrac{|x_n| \times \overline{f}_{[0,|x_n|]}}{x_2 \times \overline{f}_{[0,x_2]}} \text{ for } x_n < 0 \text{ (spray nozzles inside the field)} \\ 1 + \dfrac{x_n \times f^{max}_{[0,x_n]}}{x_2 \times \overline{f}_{[0,x_2]}} \text{ for } x_n > 0 \text{ (spray nozzles outside the field)} \end{cases} \quad (12)$$

When the spray nozzles are located inside the field, $r_{dep,mass}(x_n) < 1$, indicating that the deposition mass of the pesticide in the off-field area should be less than that of the default scenario (where spray nozzles are located at the field edge). In contrast, when the spray nozzles are located outside the field, $r_{dep,mass}(x_n) > 1$.

3. Results and discussions

3.1. Cumulative mass drift deposition fraction curves

Fig. 3 illustrates the mass cumulative drift deposition fraction (mass deposited per unit mass applied) curves based on the selected drift functions generated by using the default settings with a field length of 100 m. We note that the drift functions have specific validity ranges, and the over-sprayer range is considered to be between the field edge and the lower validity limit for specific drift functions, where we assume that this area is receiving 100% of applied pesticide deposition fraction, which is in fact overspray rather than actual drift. The deposition area is

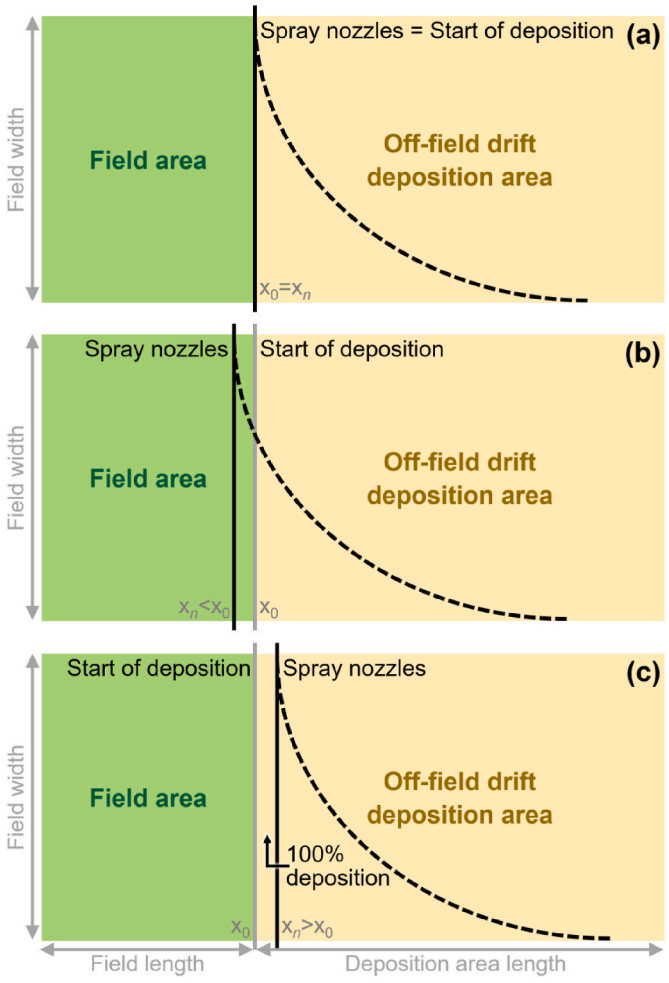

Fig. 2. Distinguishing three cases for determining where drift deposition starts and ends according to experimental drift functions. (a) The spray nozzle position, x_n, is located at the field edge, x_0. (b) The spray nozzles are located within the treated field. (c) The spray nozzles are located outside the treated field.

defined to extend up to the upper validity limit per drift function. The conversion of mass fractions to percent by multiplying fraction values with 100 was used to better illustrate very small values.

In Bueno et al., 2017), the drift curves for beans are found to follow an exponential function (eq. (3d)) with a validity range between 2.5 and 50 m for boom sprayer applications. The resulting cumulative drift deposition mass fraction is calculated using eq. (6d) (Fig. 3a). When boom sprayers are compared, the application of finer droplets resulted in a slightly higher drift deposition fraction (2.88%) than medium-size droplets (2.73%). For soybeans, the calculated cumulative drift fraction using similar boom sprayer application methods ranges from 2.54% to 2.56% (Fig. 3a), which is lower than drift fractions found for beans. Similarly, the use of boom sprayer with finer droplets results in higher emissions than with medium-size and coarse droplets.

If setting a buffer zone of 3 m along the field edge, which is not itself included in the deposition area, the cumulative drift deposition fraction dropped to 0.21% to 0.35% for beans using boom sprayer and to 0.04% to 0.06% for soybeans using boom sprayer (Fig. 3b), which is a factor of 10 to 60 lower than the cumulative drift deposition fraction without buffer zones.

For soybeans with aerial application, the deposition area is larger with higher validity limit till 300 m and the drift deposition fraction can be as high as 20% to 60% based on different nozzle types and positions (Fig. 3c). A 90-degree nozzle lead to the highest drift deposition fraction and the rotary atomizer resulted in the lowest fraction.

When testing cumulative drift deposition mass fractions for grapes (Fig. 3d), most of the drift curves followed a power function (eq. (3a)) except for air induction hollow cone spray TVI nozzles, which followed an exponential function (eq. (3d)) (Codis and Bos, 2011; Ganzelmeier and Rautmann, 2000). When using canon spider vault sprayer, the highest emission was found at 4.83%, while the emission for the rest of the application techniques ranged from 3.06% to 3.71%. Air-assisted sprayers resulted in higher drift deposition fraction than those without air-assistance.

For potatoes (Fig. 3f), boom sprayers with different settings, including drift reduction equipment, were tested, and related drift curves followed an exponential function (eq. (3d)) (Holterman and van de Zande, 2003), resulting in a cumulative drift deposition fraction between 1% and 1.2%. Knapsack sprayers were also tested (García-Santos et al., 2016), with a cumulative drift deposition fraction of 0.83% mainly due to the lower validity limit and validity range (0.5 m to 20 m) (i.e. a smaller deposition area). Different drift reduction techniques for boom sprayers, such as raised booms, air assistance, and drift reduction nozzles, reduced cumulative drift deposition fractions from 1.2% to 1%, with raised boom having the least emission.

In the case of cotton drift deposition (Fig. 3e), hand-operated sprayers and centrifugal cane sprayers were tested at different heights (1 m and 1.5 m). The drift fraction was found to be significantly higher when using the centrifugal cane sprayer than the hand-operated sprayer (Gouda et al., 2018). The drift deposition fraction ranged from 0.64% to 0.77% for the knapsack sprayer and increased to 1.42% to 2.12% for the centrifugal cane sprayer.

We note that drift deposition fractions are usually higher for fruit trees (Fig. 3g) than for other crops, and the early stage of application results in a higher drift fraction (4.15% to 4.25%) as compared to late-stage application (3.35% to 3.50%), mainly due to the different coverage of leaves (Holterman and van de Zande, 2003).

The cumulative drift deposition mass fraction in coffee crops ranges between 2.74% and 2.88% (Fig. 3g), depending on the application technique. On the other hand, crops such as olives, sugar beets, and cereals exhibit lower drift deposition fractions ranging from 0.08% to 0.31% (Fig. 3h).

According to eq. (10), the cumulative drift deposition mass fraction depends on the ratio of A_{dep}/A_{field} where the field area and off-field deposition area share the same field width. To examine the impact of the field length on emission, different field lengths from 10 m to 1000 m were tested, and the drift function on coffee using an air blast sprayer with standard ATR nozzles and on grapes using canon spider vault were selected as examples. The cumulative drift deposition mass fraction for the whole deposition area was found to be 28.8% when the field length was set to 10 m, and 0.29% when set to 1000 m for coffee, and 0.48% to 48.3% for grapes, indicating a simple exponential decrease.

In general, drift deposition fractions are less than 3% when setting the field length at 100 m, with the exception of grapes/vines and fruit trees, where the drift fractions can be as high as 4% to 5% when using canon or air blast sprayers, respectively, and the fractions can be up to 20% to 60% when using the aerial application. We acknowledge that the drift deposition fractions generated by different application methods exhibit substantial variations, and the effects of various techniques, such as raised booms, air assistance, and drift reduction nozzles, drive these variations. Setting of buffer zones along field edge can compensate the drift deposition related emissions into non-treated deposition areas in cases where such buffer zones are considered part of the treated field (Gentil-Sergent et al., 2022; Gentil et al., 2020a).

3.2. Drift deposition between field edge and lower drift function validity limit

Deposition fractions are usually not reported in experimental drift deposition studies for the area related to the distance between the actual field edge and the lower validity limit of a given function. We, hence,

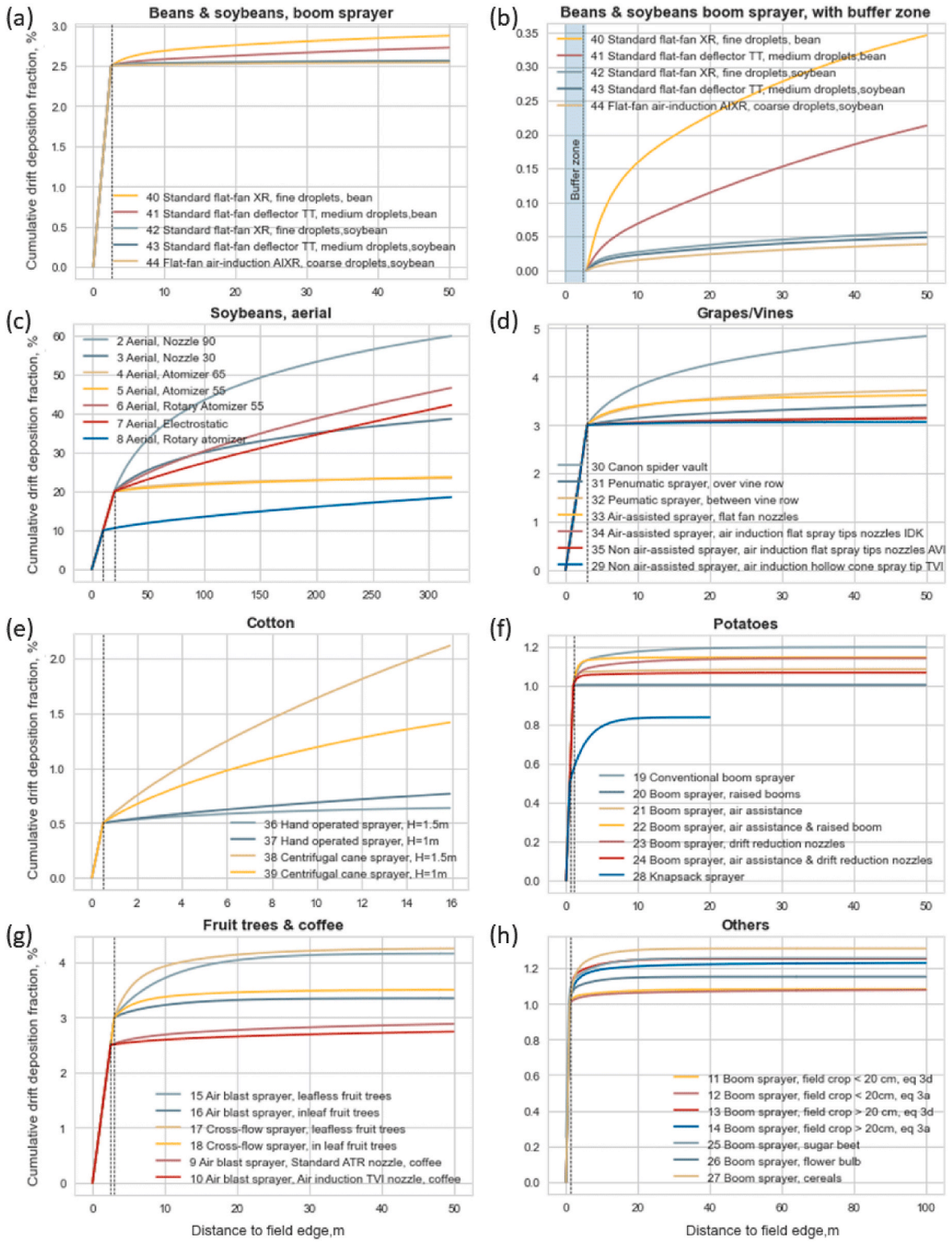

Fig. 3. Cumulative drift deposition fractions of pesticides (mass deposited per unit mass applied, multiplied by 100 to be expressed in %), plotted as function of the distance from the field edge, with default field length along the field edge set to 100 m for (a) soybeans and beans, (b) soybeans and beans with 3 m buffer zone, (c) soybeans, (d) grapes/vines, (e) cotton, (f) potatoes, (g) fruit trees, and (h) other crops. Blue dashed line represents the position of the lower validity limit of the experimental drift function, and the straight-line part between field edge ($x = 0$ m) to lower validity limit represents the overspray region between the field edge and the lower validity limit. Blue shaded area represents a buffer zone. (For interpretation of the references to colour in this figure legend, the reader is referred to the Web version of this article.)

tested different assumptions for this area, such as possible overspray, i.e. receiving 100% deposition fraction. Our results indicate that different assumptions on the drift deposition between field edge and lower validity limit of a given drift function clearly impact final cumulative drift deposition fractions as discussed in the following.

Assumption 1. For fruit tree deposition curves, which follow an exponential function (eq. (3d)) with a lower validity limit of $z_2 = 3$ m to a far edge $z_2 = 50$ m, when the distance between the field edge and lower validity limit receives 100% deposition fraction, the final cumulative drift deposition fraction is 3.35% to 3.5% for application on fruit trees with leaves and 4.15% to 4.25% for application on leafless fruit trees (Fig. 4a). Drift deposition is slightly higher for cross-flow sprayers compared to air-blast sprayers.

Assumption 2. When extrapolating deposition fractions between field edge and lower validity limit directly from the underlying drift functions, the cumulative drift deposition fraction is lower as compared to assuming 100% deposition. For application on fruit trees without leaves, it ranges from 2.59% to 3.4%, and for application on fruit trees with leaves, it ranges from 1.05% to 1.36% (Fig. 4b).

Assumption 3. Finally, we consider a linear interpolation for the deposition from 100% at the field edge to deposition fraction at the lower validity limit derived directly from the underlying drift function (Fig. 4c). The related cumulative drift deposition fraction ranges from 2.94% to 3.29% for application on fruit trees without leaves and 1.95% to 2.21% for application on fruit trees with leaves.

All in all, the cumulative drift deposition fraction varies depending on the assumptions made for the deposition between the field edge and the lower validity limit of the underlying drift curves. In this study, we suggest using a conservative assumption that the drift deposition is equivalent to 100% of the application rate in the range below the lower validity limit. Since it is challenging to determine precisely how much is deposited between the field edge and the lower validity limit of any fitted drift function, alternative approaches like mechanistic drift deposition models might be needed to provide more realistic estimates, which we discuss in our last results section.

3.3. Impact of the spray nozzles position on estimated deposition mass

The lower validity limit of a given drift function can lead to substantial impacts on cumulative drift deposition pesticide mass fractions, as illustrated in Fig. 3b. As discussed in the previous section, the deposition mass of the pesticide in the off-field area is influenced by the assumption for drift deposition over the area between the field edge and the function's lower validity limit, which can result in either overestimation or underestimation of drift deposition.

We analyzed the impact of nozzle positions relative to the field edge

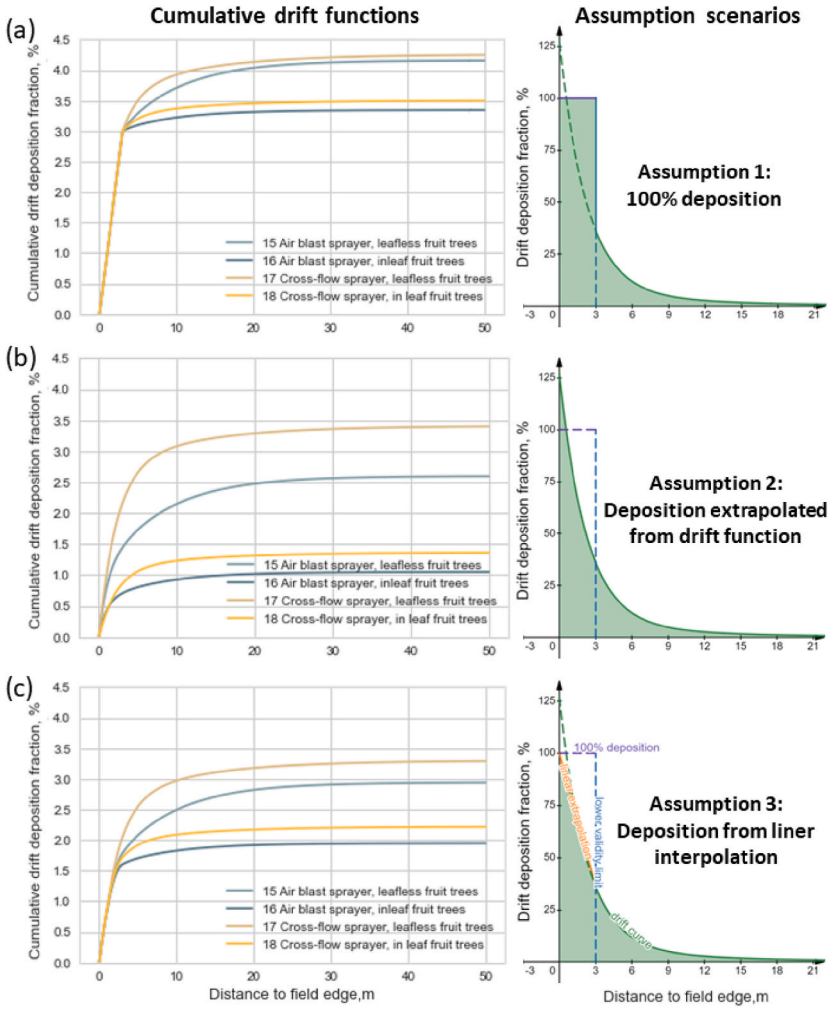

Fig. 4. Cumulative drift deposition fractions of pesticides (mass deposited per unit mass applied, multiplied by 100 to be expressed in %), plotted as a function of distance from the field edge, with field length along he field edge set to 100 m for fruit trees (left), and illustrations of underlying drift curves with green shaded area representing the cumulative drift deposition mass fraction (right) based on three assumptions. (For interpretation of the references to colour in this figure legend, the reader is referred to the Web version of this article.)

on drift deposition mass for real-world cases. Fig. 5 displays $r_{dep,mass}$ values from eq. (12) for the example drift functions for cotton using hand operated sprayer and centrifugal cane sprayer. The ratio of $m_{dep,real}(x_n)$ to $m_{dep,real}(0)$, denoted as $r_{dep,mass}$, is plotted against x_n at a range of [− 3, 3] meters. The three scenarios build on different assumptions. In the first scenario, drift deposition starts with the spray nozzles at the actual field edge (i.e. the line between the treated field and the non-treated area outside the field, referred to as deposition area). In the second scenario, spray nozzles are assumed to be entirely within the treated field; with that, part of the drift deposition is not reaching the considered deposition area. In the third scenario, spray nozzles are assumed to reach into the deposition area. For further details, see Sections 2.3 and 2.5. Based on these scenarios, results show that setting the spray nozzles within the treated field ($x_n < 0$) can result in a deposition mass ratio of <1, indicating that the estimated drift deposition mass of the pesticide in the off-field area would be lower than the default estimate when the spray nozzles are set at the field edge. The ratio ranges from 0.58 to 1 for centrifugal cane sprayers at spray height H= 1.5 m, 0.46 to 1 for centrifugal cane sprayers at spray height H= 1 m, and 0.14 to 1, 0.26 to 1 for hand operated sprayer at sprayer height H= 1.5 m and H= 1 m. The turning point from Fig. 5 are due to the lower validity limit of 0.5 m that after the x= −0.5 m point, the deposition area will start to receive 100% deposition (Fig. 4a). These results indicate that if the spray nozzles are set within the treated area, a substantial overestimation of pesticide deposition mass can occur when assuming the spray nozzles to be at the field edge (see Fig. 2b). This demonstrates that setting a buffer zone within the treated field (close to the field edge) can effectively reduce pesticide deposition mass emitted to off-field areas.

In contrast, setting the spray nozzles outside of the field can lead to an underestimation of the pesticide deposition mass in the off-field area when assuming the spray nozzles to be at the field edge (see Fig. 2c). For instance, when the nozzles are set at 3 m outside the field edge, the mass ratio $r_{dep,mass}$ is 2.41 for centrifugal cane sprayers at H= 1 m, 3.11 for centrifugal cane sprayers at H= 1 m, 4.91 for hand-operated sprayers at H= 1 m, and 5.72 for hand-operated sprayers at H= 1.5 m. The overspray of the pesticide is deposited between the field edge and the nozzles outside the field, leading to a higher degree of error in the emission estimation compared to the influence of the nozzles being positioned within the treated field.

3.4. Comparison with previous emission estimation approaches

Fig. 6 presents a comparison of our approach to derive drift deposition mass fractions with the approach followed in PestLCI 1.0 (Birkved and Hauschild, 2006). The experimental drift curve used for this comparison was proposed for pesticides applied via conventional spray equipment on field crops (lower than 1 m) with a function of $f(x)$= 0.1707×$e^{-0.0958}$ (Birkved and Hauschild, 2006; EPPO, 1996). In the previous study, the drift deposition fraction was calculated by summing up the mass lost spray swath and setting the first swath to the distance equal to half the width of the spray boom plus the width of the protective no-spray zone. This approach is heavily dependent on the number of passes and the width of each spray swath (for details, see Supplementary Materials, Section S1.2), yet not corresponding to the usual setup of deriving experimental drift functions that are typically derived from a sufficiently high and not stated number of swaths beyond which no additional (relevant) deposition is seen.

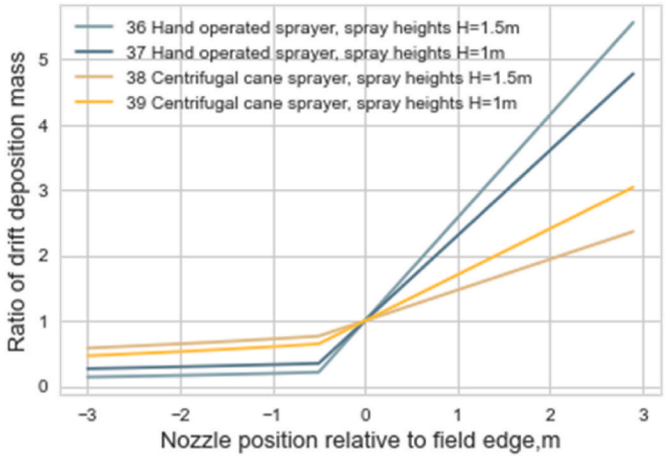

Fig. 5. Ratio of deposition mass with different nozzle positions ranging from −3 m (inside the field) to 3 m (outside the field) relative to the field edge and deposition mass for nozzles at directly at field edge (default case), for cotton drift functions (Gouda et al., 2018) as example.

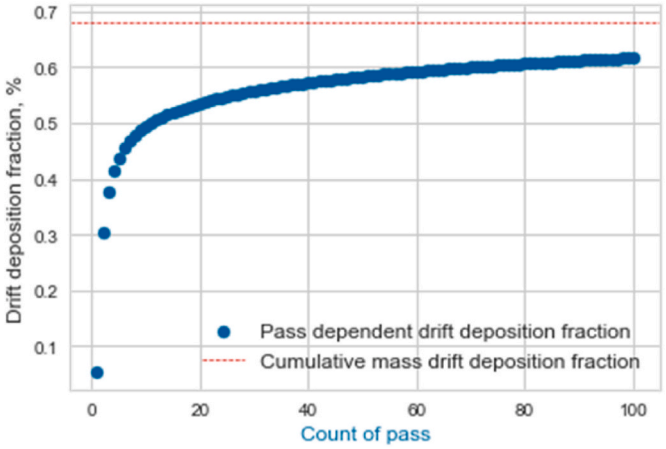

Fig. 6. Drift deposition fractions (mass deposited per unit mass applied, multiplied by 100 to be expressed in %) derived from two models based on the underlying drift curve $f(x) = 0.1707 \times e^{-0.0958}$ for pesticides applied via conventional spray equipment on field crop (Birkved and Hauschild, 2006; EPPO, 1996). Dots represent swath-dependent drift deposition fraction as a function of the number of passes of spray swath considered (not applicable for cumulative emission estimation). Line graph represents cumulative drift deposition pesticide mass fraction for the whole deposition area (applicable for cumulative emission estimation).

Wind drift is usually relevant within distances of up to 100 m. Hence, pass numbers ranging from 1 to 100 (with respective sprayer width from 100 to 1 m) are tested to obtain the sum of deposition fractions of single pass of spray swath. The results show that as the number of passes increases, the sum of deposition fractions (i.e., the cumulative result) also increases, reaching a limit of around 0.61%. However, the deposition fraction calculated using the same underlying drift function but based on the integral cumulative mass deposited over the relevant deposition area proposed in this study was calculated based on the distance from the field edge and reached 0.68% at the upper validity limit, 100 m. This value is larger than the value calculated by the previous approach, due to the integrity required for the number of spray passes. The deposition fraction calculated by the previous approach increases as the number of spray passes increases, for instance, when only five spray passes were used, the cumulative deposition fraction was 0.4%, which is roughly 60% of the simulation results obtained from the proposed approach in this study. The discrete-simulation approach adopted by the PestLCI model is affected by the pass number and characteristics of spray swath which is usually not given in drift experiments as they spray as many passes as needed to not get additional drift in deposition area. In contrast, the proposed model in this study directly calculates the f_{dep} value by linking the mass deposition fraction (or fraction lost by wind) to the drift deposition function (the experimental curve) that can better interpret the physical process of the drift deposition and performs a precise simulation.

The previous discrete point estimates further underestimate the drift deposition fraction (Fig. 6) when the spray swath width is large because the pass number of the spray swath will decrease and fewer discrete points will be chosen to be summed up, leading to an underestimation of the overall emissions. To accurately analyze the overall emissions deposited on the relevant deposition area from a given pesticide application scenario, the cumulative deposition fraction using the integral of the drift deposition function is the correct approach (see also Fig. 1).

3.5. Alternative drift deposition approaches and future research needs

Both, our proposed and the previously applied approach assumed a square-shaped treated field, which can simplify the simulation. However, in real-world scenarios, crop fields typically have mostly a rectangular shape, where the square shape is a special case. The structure of the rectangular shape (i.e. the length-to-width ratio) could substantially affect the simulated deposition fraction values. For example, if the length of the treated field (i.e. parallel to the wind direction) is shorter than the width of the field, the simulated deposition fraction should be higher than that simulated for the square-shaped field. This is due to that the longer path passed by the spray swaths, with a larger pesticide fraction that will be carried by wind drift and transported to the off-field drift deposition area, resulting in underestimating the mass fraction of the pesticide deposited in the off-field area. Thus, we recommend considering the length-to-width ratio of the treated field as input variable to improve drift deposition estimates for rectangular-shaped fields. In addition, in real-world scenarios, the wind direction may not be vertical to the path of the spray swaths. With that, the orthogonal decomposition of the vector of the drift deposition function should be considered. Thus, we also recommend adding the angle between the wind direction and the path of the spray swaths as variable into the proposed model, which can improve the interpretation and application of the drift deposition function.

Currently, the predominantly applied drift models in comparative impact assessment are data-driven (i.e. derived from experimental drift functions that are specific to certain crops and application techniques). As discussed above, such models have strong limitations in terms of field shape, drift curve fitting, and transferability to other crops and pesticide application settings. This is due to specific environmental conditions, crops, and application methods and techniques that are considered in drift experiments, which restricts their ability to account for variations in factors, such as wind speed and direction, temperature and evaporation, crop interception, foliage density, and droplet characteristics. Moreover, obtaining data on the amount of pesticide deposited between the field edge and the lower validity limit of drift functions is challenging, leading to different assumptions and resulting in varying cumulative drift deposition fractions. In this study, we assumed that for the experimental drift curves, the deposition started at nozzle position at field edge. However, if field measurements are located too far away from the nozzles, this approximation could magnify the uncertainty of the simulation results. To address this issue, users can either incorporate a piecewise function into the data-driven method to account for this non-measurement distance (using either the drift function or linear approach), or develop mechanistic approaches to generate drift functions starting from the position of the last nozzle. Consequently, this variability can lead to either overestimation or underestimation of the overall mass of pesticide deposited in off-field areas.

At present, most drift functions are developed and studied for spray booms, without taking into account other significant types of pesticide application methods, such as using aircraft and personal equipment (directed spray). Aircraft, particularly drones, are commonly used to improve the efficiency of pesticide application (i.e., in terms of timeliness) in modern agriculture. On the other hand, personal equipment is also required as a directed-spray method to deliver pesticides to specific parts of plants. These pesticide application methods exhibit different conditions of pesticide emission from the treated field, such as altitude, quantity, and spray angles (Wei et al., 2020). As a result, the corresponding drift functions will differ from those derived for spray booms. To address this issue, a generalized mechanistic model is needed that can describe cumulative pesticide emission processes between the treated field and off-field areas. Such a model should take into account several key variables, including initial conditions (i.e., pesticide application), environmental factors (e.g., temperature, humidity, and wind characteristics), field conditions (e.g., field shape and slope), crop varieties (e.g., plant height and phenotype), and spray solution formulas (e.g., droplet size and density). Additionally, drift functions aim to characterize the fraction of pesticides depositing in off-field areas. Therefore, not only should the initial pesticide drift (i.e., deposition fraction) immediately following pesticide application be considered, but also any relevant subsequent processes that influence ultimate pesticide emission distribution, including volatilization from the treated field (e.g., pesticide residues on plant surfaces relevant for crop uptake and related human exposure (Fantke et al., 2012; Fantke and Jolliet, 2016). This issue can be resolved by incorporating pesticide drift functions (considered as an initial mass fraction solution) and pesticide fate models (considered as a time-dependent mass fraction solution). Thus, in future studies, a generalized mechanistic model as well as the integration of pesticide fate models are promising for addressing emissions and related impacts of pesticide drift from treated fields to off-field areas.

Therefore, alternative methods are necessary to estimate off-field emissions and generate drift deposition fractions that can encompass a broader range of environmental conditions, application methods and techniques, and crop varieties. Promising mechanistic models that could be adapted to derive cumulative emission fractions are the Casanova drift model (Casanova et al., 2022) and the SiMod model (Butler Ellis and Miller, 2010), which incorporate various factors, including droplet transport and evaporation, horizontal wind profiles, droplet size distribution, and canopy effects on arable crops. By employing such approaches, it becomes possible to obtain cumulative drift deposition fractions that are applicable to a wider range of environmental conditions, application methods and techniques, and crops across the entire deposition area, which is an important element in evaluating pesticide emissions and related impacts in support of reducing related chemical pollution.

4. Conclusions

In this study, we proposed a modelling approach to quantify drift deposition fractions of pesticide (or mass fraction lost by wind drift via deposition) for use in impact assessment contexts, based on the integral form of the drift deposition function obtained from experimental data. The proposed model can be flexibly adjusted according to the position of the spray nozzles to avoid underestimating or overestimating the mass of the pesticide deposited in the off-field area. In addition, we compared the simulated deposition fractions with that applied in earlier mass balanced approaches for impact assessments. The comparison results indicated that our proposed model is more suitable for deriving cumulative emissions associated with drift deposition of pesticides. To overcome current limitations of emission models based on drift experiments, we recommend to employ mechanistic drift models that allow to account for field, crop and application characteristics, and with that may cover a wider range of real-world pesticide application scenarios in comparative impact assessment.

CRediT authorship contribution statement

Yuyue Zhang: Formal analysis, Methodology, Validation, Visualization, Writing - original draft. **Zijian Li:** Methodology, Writing - review & editing. **Stefan Reichenberger:** Methodology, Writing - review & editing. **Céline Gentil-Sergent:** Conceptualization, Methodology, Writing - review & editing. **Peter Fantke:** Conceptualization,

Methodology, Project administration, Supervision, Visualization, Writing - original draft.

Declaration of competing interest

The authors declare that they have no known competing financial interests or personal relationships that could have appeared to influence the work reported in this paper.

Data availability

No data was used for the research described in the article.

Acknowledgements

We thank Carlos Melero for supporting the compilation of experimental drift functions, as well as Anja Gladbach and Andrew Chapple for input on alternative drift deposition modelling approaches. This work was supported by the 'Crop Protection Environmental Impact Reduction' project funded by the Bayer AG, Germany; and by the SAGROPIA project (grant agreement no. 101136677) funded under the European Union's Horizon Europe Research and Innovation program.

Appendix A. Supplementary data

Supplementary data to this article can be found online at https://doi.org/10.1016/j.envpol.2023.123135.

References

Aurisano, N., Huang, L., Milà i Canals, L., Jolliet, O., Fantke, P., 2021. Chemicals of concern in plastic toys. Environ. Int. 146 https://doi.org/10.1016/j.envint.2020.106194.

Bach, M., Guerniche, D., Thomas, K., Trapp, M., Kubiak, R., Hommen, U., Klein, M., Reichenberger, S., Pires, J., Preuß, T., 2017. Bewertung des Eintrags von Pflanzenschutzmitteln in Oberflächengewässer – Runoff, Erosion und Drainage. German Federal Environment Agency, Dessau.

Birkved, M., Hauschild, M.Z., 2006. PestLCI-A model for estimating field emissions of pesticides in agricultural LCA. Ecol. Model. 198, 433–451. https://doi.org/10.1016/j.ecolmodel.2006.05.035.

Bueno, M.R., Cunha, J.P.A.R.d., de Santana, D.G., 2017. Assessment of spray drift from pesticide applications in soybean crops. Biosyst. Eng. 154, 35–45. https://doi.org/10.1016/j.biosystemseng.2016.10.017.

Butler Ellis, M.C., Miller, P.C.H., 2010. The Silsoe Spray Drift Model: a model of spray drift for the assessment of non-target exposures to pesticides. Biosyst. Eng. 107, 169–177. https://doi.org/10.1016/j.biosystemseng.2010.09.003.

Casanova, E., Pai, N., Chapple, A.C., Gao, Z., Isemer, R., 2022. The Casanova Drift Model : an arable crop boom spray drift model. In: Aspects 147: International Advances in Pesticide Application, pp. 95–104.

Codis, S., Bos, C., 2011. Réduction de la dérive, 8 matériels testés sur vigne. Phytoma 640, 1–5.

Dijkman, T.J., Birkved, M., Hauschild, M.Z., 2012. PestLCI 2.0: a second generation model for estimating emissions of pesticides from arable land in LCA. Int. J. Life Cycle Assess. 17, 973–986. https://doi.org/10.1007/s11367-012-0439-2.

EFSA, 2020. Scientific report of EFSA on the 'repair action' of the FOCUS surface water scenarios. EFSA J. https://doi.org/10.2903/j.efsa.2020.6119.

EPPO, 1996. Chapter 12: air in "Decision-making scheme for the environmental risk assessment of plant protection products" (draft version). Eur. Mediterr. Plant Prot. Organ. Counc. Eur. 96, 5543.

Fantke, P., Aurisano, N., Bare, J., Backhaus, T., Bulle, C., Chapman, P.M., De Zwart, D., Dwyer, R., Ernstoff, A., Golsteijn, L., Holmquist, H., Jolliet, O., McKone, T.E., Owsianiak, M., Peijnenburg, W., Posthuma, L., Roos, S., Saouter, E., Schowanek, D., van Straalen, N.M., Vijver, M.G., Hauschild, M., 2018a. Toward harmonizing ecotoxicity characterization in life cycle impact assessment. Environ. Toxicol. Chem. 37, 2955–2971. https://doi.org/10.1002/etc.4261.

Fantke, P., Aylward, L., Bare, J., Chiu, W.A., Dodson, R., Dwyer, R., Ernstoff, A., Howard, B., Jantunen, M., Jolliet, O., Judson, R., Kirchhübel, N., Li, D., Miller, A., Paoli, G., Price, P., Rhomberg, L., Shen, B., Shin, H.M., Teeguarden, J., Vallero, D., Wambaugh, J., Wetmore, B.A., Zaleski, R., McKone, T.E., 2018b. Advancements in life cycle human exposure and toxicity characterization. Environ. Health Perspect. 126, 1–10. https://doi.org/10.1289/EHP3871.

Fantke, P., Chiu, W.A., Aylward, L., Judson, R., Huang, L., Jang, S., Gouin, T., Rhomberg, L., Aurisano, N., McKone, T., Jolliet, O., 2021. Exposure and toxicity characterization of chemical emissions and chemicals in products: global recommendations and implementation in USEtox. Int. J. Life Cycle Assess. 26, 899–915. https://doi.org/10.1007/s11367-021-01889-y.

Fantke, P., Huang, L., Overcash, M., Griffing, E., Jolliet, O., 2020. Life cycle based alternatives assessment (LCAA) for chemical substitution. Green Chem. 22, 6008–6024. https://doi.org/10.1039/d0gc01544j.

2001 FOCUS, 2001. FOCUS surface water scenarios in the EU evaluation process under 91/414/EEC. Report of the FOCUS working group on surface water scenarios, EC Document Reference SANCO/4802/2001-rev.2. 245 pp.

Fantke, P., Illner, N., 2019. Goods that are good enough: introducing an absolute sustainability perspective for managing chemicals in consumer products. Curr. Opin. Green Sustainable Chem. 15, 91–97. https://doi.org/10.1016/j.cogsc.2018.12.001.

Fantke, P., Jolliet, O., 2016. Life cycle human health impacts of 875 pesticides. Int. J. Life Cycle Assess. 21, 722–733. https://doi.org/10.1007/s11367-015-0910-y.

Fantke, P., Wieland, P., Juraske, R., Shaddick, G., Itoiz, E.S., Friedrich, R., Jolliet, O., 2012. Parameterization models for pesticide exposure via crop consumption. Environ. Sci. Technol. 46, 12864–12872. https://doi.org/10.1021/es301509u.

Ganzelmeier, H., Rautmann, D., 2000. Drift, drift reducing sprayers and sprayer testing. Aspect Appl. Biol. 57, 1–10.

García-Santos, G., Feola, G., Nuyttens, D., Diaz, J., 2016. Drift from the use of hand-held knapsack pesticide sprayers in Boyacá (Colombian Andes). J. Agric. Food Chem. 64, 3990–3998. https://doi.org/10.1021/acs.jafc.5b03772.

Gentil-Sergent, C., Basset-Mens, C., Gaab, J., Mottes, C., Melero, C., Fantke, P., 2021. Quantifying pesticide emission fractions for tropical conditions. Chemosphere 275. https://doi.org/10.1016/j.chemosphere.2021.130014.

Gentil-Sergent, C., Basset-Mens, C., Renaud-Gentié, C., Mottes, C., Melero, C., Launay, A., Fantke, P., 2022. Introducing ground cover management in pesticide emission modeling. Integrated Environ. Assess. Manag. 18, 274–288. https://doi.org/10.1002/ieam.4482.

Gentil, C., Basset-Mens, C., Manteaux, S., Mottes, C., Maillard, E., Biard, Y., Fantke, P., 2020a. Coupling pesticide emission and toxicity characterization models for LCA: application to open-field tomato production in Martinique. J. Clean. Prod. 277, 124099 https://doi.org/10.1016/j.jclepro.2020.124099.

Gentil, C., Fantke, P., Mottes, C., Basset-Mens, C., 2020b. Challenges and ways forward in pesticide emission and toxicity characterization modeling for tropical conditions. Int. J. Life Cycle Assess. 25, 1290–1306. https://doi.org/10.1007/s11367-019-01685-9.

Gouda, A.-I., Mehoba, M.H.L., Toko, I.I., Scippo, M.-L., Kestemont, P., Schiffers, B., 2018. Comparaison de la dérive pour deux types de pulvérisateurs utilisés en production cotonnière au Bénin. Base 22, 94–105. https://doi.org/10.25518/1780-4507.16431.

Hauschild, M.Z., Rosenbaum, R.K., Olsen, S.I., 2018. Life Cycle Assessment. Springer International Publishing, Cham. https://doi.org/10.1007/978-3-319-56475-3.

Hernández-Hernández, C.N.A., Valle-Mora, J., Santiesteban-Hernández, A., Bello-Mendoza, R., 2007. Comparative ecological risks of pesticides used in plantation production of papaya: application of the SYNOPS indicator. Sci. Total Environ. 381, 112–125. https://doi.org/10.1016/j.scitotenv.2007.03.014.

Holterman, H.J., van de Zande, J.C., 2003. IMAG Drift Calculator, v1.1, User Manual.

Holterman, H.J., van de Zande, J.C., Huijsmans, J.F.M., Wenneker, M., 2017. An empirical model based on phenological growth stage for predicting pesticide spray drift in pome fruit orchards. Biosyst. Eng. 154, 46–61. https://doi.org/10.1016/j.biosystemseng.2016.08.016.

Holterman, H.J., van der Zande, J.C., Huijsmans, J.F.M., Wenneker, M., 2018. Development of a Spray Drift Model for Spray Applications in Fruit Orchards. Wageningen Research. https://doi.org/10.18174/442091. Report WPR-566. 72pp.

ISO, 2005. ISO 22866 International Standard. Equipment for Crop Protection - Methods for Field Measurement of Spray Drift. International Organization for Standardization.

Jolliet, O., Huang, L., Hou, P., Fantke, P., 2021. High throughput risk and impact screening of chemicals in consumer products. Risk Anal. 41, 627–644. https://doi.org/10.1111/risa.13604.

Kosnik, M.B., Hauschild, M.Z., Fantke, P., 2022. Toward assessing absolute environmental sustainability of chemical pollution. Environ. Sci. Technol. 56, 4776–4787. https://doi.org/10.1021/acs.est.1c06098.

Nemecek, T., Antón, A., Basset-Mens, C., Gentil-Sergent, C., Renaud-Gentié, C., Melero, C., Naviaux, P., Peña, N., Roux, P., Fantke, P., 2022. Operationalising emission and toxicity modelling of pesticides in LCA: the OLCA-Pest project contribution. Int. J. Life Cycle Assess. 27, 527–542. https://doi.org/10.1007/s11367-022-02048-7.

Owsianiak, M., Hauschild, M.Z., Posthuma, L., Saouter, E., Vijver, M.G., Backhaus, T., Douziech, M., Schlekat, T., Fantke, P., 2023. Ecotoxicity characterization of chemicals: global recommendations and implementation in USEtox. Chemosphere 310. https://doi.org/10.1016/j.chemosphere.2022.136807.

Persson, L., Carney Almroth, B.M., Collins, C.D., Cornell, S., de Wit, C.A., Diamond, M.L., Fantke, P., Hassellöv, M., MacLeod, M., Ryberg, M.W., Søgaard Jørgensen, P., Villarrubia-Gómez, P., Wang, Z., Hauschild, M.Z., 2022. Outside the safe operating space of the planetary boundary for novel entities. Environ. Sci. Technol. 56, 1510–1521. https://doi.org/10.1021/acs.est.1c04158.

Rautmann, D., Streloke, M., Winkler, R., 2001. New basic drift values in the authorization procedure for plant protection products. Mitteilungen aus der Biol. Bundesanstalt für L. 388, 133–141.

Reichenberger, S., Bach, M., Skitschak, A., Frede, H.G., 2007. Mitigation strategies to reduce pesticide inputs into ground- and surface water and their effectiveness; A review. Sci. Total Environ. 384, 1–35. https://doi.org/10.1016/j.scitotenv.2007.04.046.

Renaud-Gentié, C., Dijkman, T.J., Bjørn, A., Birkved, M., 2015. Pesticide emission modelling and freshwater ecotoxicity assessment for grapevine LCA: adaptation of PestLCI 2.0 to viticulture. Int. J. Life Cycle Assess. 20, 1528–1543. https://doi.org/10.1007/s11367-015-0949-9.

Rosenbaum, R.K., Anton, A., Bengoa, X., Bjørn, A., Brain, R., Bulle, C., Cosme, N., Dijkman, T.J., Fantke, P., Felix, M., Geoghegan, T.S., Gottesbüren, B., Hammer, C., Humbert, S., Jolliet, O., Juraske, R., Lewis, F., Maxime, D., Nemecek, T., Payet, J., Räsänen, K., Roux, P., Schau, E.M., Sourisseau, S., van Zelm, R., von Streit, B., Wallman, M., 2015. The Glasgow consensus on the delineation between pesticide emission inventory and impact assessment for LCA. Int. J. Life Cycle Assess. 20, 765–776. https://doi.org/10.1007/s11367-015-0871-1.

Tang, L., Hayashi, K., Inao, K., Birkved, M., Bruun, S., Kohyama, K., Shimura, M., 2020. Developing a management-oriented simulation model of pesticide emissions for use in the life cycle assessment of paddy rice cultivation. Sci. Total Environ. 716, 137034 https://doi.org/10.1016/j.scitotenv.2020.137034.

Tarasova, N., Makarova, A., Fantke, P., Shlyakhov, P., 2018. Estimating chemical footprint: contamination with mercury and its compounds. Pure Appl. Chem. 90, 857–868. https://doi.org/10.1515/pac-2017-1102.

van de Zande, J.C., Rautmann, D., Holterman, H.J., Huijsmans, J.F.M., 2015. Joined Spray Drift Curves for Boom Sprayers in The Netherlands and Germany, Plant Research International, Part of Wageningen UR Business Unit Agrosystems. Report 526. https://edepot.wur.nl/353554.

von Borries, K., Holmquist, H., Kosnik, M., Beckwith, K., Jolliet, O., Goodman, J., Fantke, P., 2023. Potential for machine learning to address data gaps in human toxicity and ecotoxicity characterization. Environ. Sci. Technol. 57, 18259–18270. https://doi.org/10.1021/acs.est.3c05300.

Wei, K., Xu, W., Liu, Q., Yang, L., Chen, Z., 2020. Preparation of a chlorantraniliprole–thiamethoxam ultralow-volume spray and application in the control of *Spodoptera frugiperda*. ACS Omega 5, 19293–19303. https://doi.org/10.1021/acsomega.0c02912.

Zijp, M.C., Posthuma, L., Van De Meent, D., 2014. Definition and applications of a versatile chemical pollution footprint methodology. Environ. Sci. Technol. 48, 10588–10597. https://doi.org/10.1021/es500629f.